arXiv:1207.4651v1 [gr-qc] 19 Jul 2012

Phenomenological Relations for Axial Quasi-normal Modes of Neutron Stars with Realistic Equations of State

J. L. Blázquez-Salcedo,[1] L. M. González-Romero,[1] and F. Navarro-Lérida[2]

[1] *Depto. Física Teórica II, Facultad de Ciencias Físicas,*
Universidad Complutense de Madrid, 28040-Madrid, Spain
[2] *Depto. Física Átomica, Molecular y Nuclear, Facultad de Ciencias Físicas,*
Universidad Complutense de Madrid, 28040-Madrid, Spain

(Dated: July 20, 2012)

Here we investigate the axial w quasi-normal modes of neutron stars for several equations of state. In particular, we study the influence of the presence of hyperons in the core of the neutron stars. We have obtained that w-modes can be used to distinguish between neutron stars with hyperons and without hyperons for compact enough stars. We present phenomenological relations for the frequency and damping times with the compactness of the neutron star for wI and wII modes showing the differences of the stars with hyperons in the core. Also, we obtain a new phenomenological relation between the real part and the imaginary part of the frequency of the w quasi-normal modes, which can be used to estimate the central pressure of the neutron stars. We are able to construct explicitly the low compactness limit configuration for which the fundamental wII mode vanishes. Finally, we have studied the influence of changes in the core-*crust* transition pressure obtaining that it is very small. To obtain these results we have developed a new method based on the Exterior Complex Scaling technique with variable angle, appropriate for the treatment of the exterior part of the quasi-normal modes, which allow us to impose constringent enough conditions to generate pure outgoing quasi-normal modes. For the interior part we use a piece-wise polytrope approximation for several equations of state. A complete study of the junction conditions have been done.

PACS numbers: 04.40.Dg, 04.30.-w, 95.30.Sf, 97.60.Jd

I. INTRODUCTION

Considerable progress has been made in the last years on the gravitational wave detectors development. Large-scale interferometric gravitational wave detectors, like LIGO, GEO, TAMA and VIRGO, have reached the original design sensitivity, and are currently beginning to operate with frequencies between 1Hz to 1kHz. The sensitivity is continuously being enhanced [1]. First detections are expected to happen within the next five years. These observations are of huge importance because they can be used to perform stringent tests of general relativity. But also because gravitational wave detection opens a new window to observations of the insights of numerous, and probably also new, astrophysical processes. Possible sources of gravitational waves are interacting black holes, coalescing compact binary systems, stellar collapses and pulsars [2].

Neutron stars are major candidates to detectable gravitational wave sources because of their rich emission spectra, that lays inside the frequency range of current detectors. A recent review about gravitational waves from neutron stars can be found in [3]. The study of the signature of the equation of state on gravitational radiation from neutron star has been developed in [4–9]. The first direct search for the gravitational-wave emission associated with oscillations of fundamental quadrupole mode excited by a pulsar glitch has been presented in [10] .

Neutron stars are found inside pulsars, and are thought to originate after the collapse of massive star cores. The supernova explosion causes violent oscillations of the resulting compact star. Similarly the coalescence of compact bodies like white dwarfs leaves behind an oscillating neutron star. The resulting excess of energy that causes the star to oscillate is radiated in the form of gravitational radiation [2].

It is well known that although the spectrum of neutron star oscillations is continuous, general perturbations causes the star to ring with concrete oscillation frequencies that dominates over the rest of possible frequencies for a certain period of time after the perturbation. These resonant frequencies can be studied introducing the concept of quasi-normal modes, that is, eigenmodes of oscillation, that, although do not form a complete set of functions in which to expand every possible perturbation evolution, are very useful in the determination of the eigenfrequencies for which the star tends to oscillate [11–13]. These eigenfrequencies are given by a complex number. The real part gives us the oscillation frequency of the mode, while the imaginary part gives us the inverse of the damping time. The quasi-normal mode spectrum is quite dependent on the properties of the star, i.e. the equation of state.

Neutron stars are compact objects of very high density. Inside of them matter is found at extreme densities ($10^{15} g/cm^3$). Current theories predict a layer structure for the neutron star, essentially composed by the core and the *crust*. The properties of the *crust* are very different from those of the core, and it is thought that this region has a solid crystalline structure similar to a metal. Although the high density matter inside the star has exotic properties, the resulting relativistic fluid that compose the neutron star can be described as a perfect fluid. What we need to know is the equation of state for the neutron star matter, but beyond the nuclear densities this relation is not well understood. The inner part of the nucleus is very model dependent, essentially because different populations of particle states may appear at those densities. The composition is not exactly known and several hypothesis exist [14, 15]. Along the core of the star and specially in the core-*crust* interface, first order phase transitions are expected to be found in realistic equations of state. These phase transitions result in small discontinuities in the energy density of the star matter [14, 16].

In order to systematize the study of constraints placed by astrophysical observations on the nature of neutron-star matter, several parameterizations of high-density equation of state (EOS) have been introduced: a piecewise polytropic approximation by Jocelyn et al. [17] and Lindblom spectral decomposition [18]. The advantage of these parameterizations is that they reduce the total amounts of parameters which modelize the equation of state to a more tractable quantity, allowing to constrain with observational data the values of the parameters, and also usually they enhance a numerical integration scheme allowing better precision. Let us note that a very large family of equations of state can be fitted to these parameterizations with a very good precision.

The detection of gravitational radiation from neutron stars can be a very useful tool to determine the neutron star equation of state. The extraction of the spectrum of quasi-normal modes (frequency and damping time) from these signals could give important constrains to the equation of state, and in consequence, information about the behavior of matter at densities beyond nuclear matter [19–25].

The theoretical study of the quasi-normal mode spectrum considering different models of neutron star with different equations of state is then well justified. The necessary formalism were developed first for quasi-normal modes of black holes by Regge and Wheeler [26] and by Zerilli [27]. Quasi-normal modes can be differentiated into polar and axial modes. In these papers it is found that the equation describing the quasi-normal mode perturbation of the Schwarzschild metric is essentially a Schrodinger like equation: the Regge-Wheeler equation for axial perturbations and the Zerilli equation for polar ones. For black holes, both types of modes are space-time modes. The formalism was studied in the context of neutron stars first by Thorne [28–32], Lindblom [33, 34], and then reformulated by Chandrasekhar and Ferrari [35–37], and Kojima [38]. In neutron stars, axial modes are purely space-time modes of oscillation (w modes), while polar modes can be coupled to fluid oscillations (although a branch of w modes can be found also in polar oscillations). In this paper we will consider only axial modes of oscillation.

The study of the quasi-normal modes spectrum is complicated because of several reasons. Quasi-normal modes can only be studied numerically. No analytical solutions are known for physically acceptable configurations of neutron stars. Another reason is that quasi-normal modes are found as isolated points scattered on the complex plane, so that usually an exhaustive scan of this plane is necessary in order to find the complete spectrum. Also the numerical study is hindered by the very definition of quasi-normal mode itself, that as we will see explicitly in the following sections, give rise to diverging functions that oscillate an infinite number of times towards spatial infinity. These functions are not well handled numerically.

Several methods have been developed to deal with these and other difficulties. For a complete review on the methods see the review by Kokkotas and Schmidt [11].

Chandrasekhar and Ferrari [35–37] used a slowly damped approximation ($\Im[\omega] \ll \Re[\omega]$), which reduces the system of equations needed to resolve the problem, so that the damping time of the quasi-normal mode can be given in terms of the real part. This method was also used in the determination of w-modes on polar perturbations of constant density neutron stars by Kojima et al [39]. It is only valid for slowly damped modes, which are present in highly compact stars, and is not appropriate for realistic configurations, although it can be used to obtain a first approximation of the fundamental frequencies.

In an interesting paper [40], Kokkotas studied the axial spectrum integrating the exterior solution up to a finite radius, which allows to impose the outgoing wave behavior to the exterior solution. The matching between the interior and exterior solutions results in the construction of a Wronskian at the matching surface, which must be zero when both solutions correspond to a quasi-normal mode.

The WKB method [41] can be used to approximate the outer solutions provided that no back-scattering is found in the exterior region. This condition usually is satisfied when the imaginary part of the mode is small compared with the real part [42].

The phase function can be studied in order to deal with the oscillatory nature of the perturbation function. Studied for black holes by Chandrasekhar and Detweiller [43], the phase function plays a fundamental role in the numerical approach made by Andersson et al in [42] and in [44] for neutron stars. The phase is usually a well behaved function if there is not back-scattering contamination in the numerical solution.

The divergence of the outgoing wave solution of the perturbation equations makes the avoidance of incoming wave contamination a difficult task. This problem was dealt for black holes by Andersson in [45] by rotating the radial variable into a complex variable parallel to the anti-Stokes line. This approach were used for constant density neutron stars in [42] and [44] together with the phase function approach. More recently, Samuelsson et al [46] used a similar complex-radius approach for a constant density configuration which dealt with the divergence at infinity by integrating the Bondi-Sachs phase along a fixed path for the complexified radius parallel to the anti-Stokes line.

Another approach is based on the Leaver continued fraction method [47], which allows to impose the outgoing wave behavior on the border of the star as a self-consistent equation that can be satisfied iteratively [48]. This method has been used successfully with realistic models of neutron stars [19, 21, 25]

As commented above, for fluid modes there is also a branch of w-modes. As these are purely space-time modes, they do not couple to matter, and the inverse Cowling approximation can be used to obtain this part of the spectrum [44].

In this work we present a new approach to calculate quasi-normal modes of realistic neutron stars. We make use of several well-known techniques, like the use of the phase for the exterior solution and the use of a complexified coordinate to deal with the divergence of the outgoing wave. We also introduce some new techniques not used before in this context: freedom in the angle of the exterior complex path of integration, a determinant algorithm to calculate the mode based on general junction conditions on the boundary of the star, implementation of 34 realistic equations of state in a piece-wise polytrope approximation, use of Colsys to integrate all the system of equations at once with proper boundary and junction conditions and possibility of implementation of phase transition discontinuities. These new techniques allow us to enhance precision, to obtain more modes in shorter times, and also to study several realistic equations of state, comparing results for different compositions.

In section II we will start presenting the well-known general formalism of quasi-normal modes. In section III we will present an study of the junction conditions for a general matching that can include first order phase transitions or surface energy layers. In most of the results of the paper we will make use of the junction conditions without phase transitions or energy layers. In section IV we describe the numerical method we have used to obtain our results, testing the algorithm to obtain already known modes for a simple model . In section V we present our results, focusing on four different equations of state: High density SLy (pure nuclear matter), ALF4 (mixed quark-nuclear matter), GNH3 and BGN1H1 (mixed hyperon-nuclear matter). In section VI we finish the paper with a summary of the main points of the work.

II. QUASI-NORMAL MODE FORMALISM

In order to fix the notation we will present a brief review of the formalism used to describe axial quasi-normal modes. In the following we use geometrized units $(c = 1, G = 1)$.

We consider an static spherical space-time with metric $ds^2 = e^{2\nu}dt^2 - e^{2\lambda}dr^2 - r^2(d\theta^2 + \sin^2\theta d\varphi^2)$. Following the original papers [28]-[38], we make perturbations over this metric, expanding the perturbation in tensor harmonics, and taking into account only the axial perturbations, i.e. those which under a parity transformation $\theta \to \pi - \theta$, $\varphi \to \pi + \phi$, transform like $(-1)^{l+1}$. Once the free gauge transformation is selected (we choose the Reege-Wheeler gauge [12]), the components of the metric perturbation are:

$$\begin{aligned} h_{t\theta} &= -h^0_{lm}\tfrac{\partial_\phi Y_{lm}}{\sin\theta}, h_{t\phi} = h^0_{lm}\sin\theta\partial_\phi Y_{lm}, \\ h_{r\theta} &= -h^1_{lm}\tfrac{\partial_\phi Y_{lm}}{\sin\theta}, h_{r\phi} = h^1_{lm}\sin\theta\partial_\phi Y_{lm}, \end{aligned} \tag{1}$$

where the angular dependence is explicitly given in terms of the spherical harmonics Y_{lm}. In general h^0_{lm} and h^1_{lm} are functions of t and r.

The matter inside of the star is considered to be a perfect fluid with stress-energy tensor $T^{\mu\nu} = (p+\rho)\,u^\mu u^\nu - pg^{\mu\nu}$, where p is the pressure, ρ is the energy density and u is the 4-velocity. Axial oscillations do not modify the energy density or the pressure of the fluid. Hence, for axial modes, inside of the star only the perturbations on the 4-velocity of the matter have to be taken into account. These perturbations are calculated considering the Lagrangian displacement vector ξ^i of the fluid, and each component of the spatial vector can also be expanded in terms of tensor harmonics. So, the Lagrangian displacement that can couple to the axial perturbations can be written as:

$$\xi^\theta = \tfrac{e^{-\nu}}{(\rho+p)r^2} W_{lm}\tfrac{\partial_\varphi Y_{lm}}{\sin^2\theta}, \tag{2}$$

$$\xi^\varphi = -\tfrac{e^{-\nu}}{(\rho+p)r^2} W_{lm}\tfrac{\partial_\theta Y_{lm}}{\sin^2\theta}, \tag{3}$$

where W_{lm} are perturbative functions of t and r, associated with the axial Lagrangian displacement. The Einstein equation $G_{\mu\nu} = 8\pi T_{\mu\nu}$ are solved considering the terms of same perturbative order and with same angular dependence.

At zero order the equations obtained are well known. Inside of the star we have:

$$\frac{dm}{dr} = 4\pi r^2\rho, \tag{4}$$

$$\frac{dp}{dr} = -(\rho+p)\frac{m + 4\pi r^3 p}{(r-2m)r}, \tag{5}$$

$$\frac{d\nu}{dr} = -\frac{1}{\rho+p}\frac{dp}{dr}, \tag{6}$$

and outside we have the Schwarzschild solution with gravitational mass M.

The equations for first order perturbation are obtained in a similar way, but they are time dependent and depend linearly in the perturbative functions. Hence, we can extract the time dependence from the functions by making a Laplace transformation:

$$\hat{f}(r,\omega) = \int_0^\infty e^{-\omega t} f(r,t)dt. \tag{7}$$

This transformation eliminates the time derivatives but introduces explicitly into the equations the eigen-value ω. After some algebraic work with the resulting equations, it can be seen that the axial perturbations must satisfy the well-known Regge-Wheeler equation [27].

$$\frac{d^2 Z^{lm}}{dr_*^2} + \left[\omega^2 - V(r)\right] Z^{lm} = 0, \tag{8}$$

where r_* is the tortoise coordinate:

$$r_* = \int_0^r e^{\lambda - \nu} dr, \tag{9}$$

and the eigen-frequency of the axial mode is a complex number $\omega = \omega_{\Re} + i\omega_{\Im}$. The equation is valid both inside the star and outside of it, and the potential can be written as:

$$V(r) = \frac{e^{2\nu}}{r^3}\left[l(l+1)r + 4\pi r^3(\rho + p) - 6m\right], \tag{10}$$

where l is the spherical harmonic index. In this work we will consider only the $l = 2$ case. Inside the star the pressure p, and the mass m are functions of r obtained by solving equations (4) -(6), and an equation of state must be provided. Outside of the star, $\rho = p = 0$ and $m = M$, the gravitational mass of the Schwarzschild metric.

Note that in general the perturbation function Z is a complex function. These translates into a set of two real second order differential equations (one for the real part $Z_{\Re}$, and another for the imaginary part $Z_{\Im}$).

Z has to satisfy a set of boundary conditions that can be obtained from the following two requirements [35]: i) the perturbation must be regular at the center of the star, and ii) the resulting quasi-normal mode must be a pure outgoing wave.

The first requirement imposes the following Taylor expansion to the Z function at the origin

$$Z = Z^{(0)} r^{l+1} + o\left(r^{l+3}\right). \tag{11}$$

Note that $Z^{(0)}$ is a non-fixed parameter, and we will make use of this freedom in our numerical method of quasi-normal mode calculation.

The second requirement imposes the quasi-normal modes to behave as purely outgoing waves at radial infinity. In general a quasi-normal mode will be a composition of incoming and outgoing waves, i.e.

$$\lim_{r_* \to \infty} Z^{in} \sim e^{i\omega r_*}, \tag{12}$$

$$\lim_{r_* \to \infty} Z^{out} \sim e^{-i\omega r_*}. \tag{13}$$

Note that, while the real part of ω determines the oscillation frequency of the wave, the imaginary part of the eigen-value determines the asymptotic behavior of the quasi-normal mode: If we call $\tau = 1/\omega_I$, the ingoing mode will behave as:

$$\lim_{r_* \to \infty} Z^{in} \sim e^{-r_*/\tau}, \tag{14}$$

which is a convergent function, and the outgoing mode:

$$\lim_{r_* \to \infty} Z^{out} \sim e^{r_*/\tau}, \tag{15}$$

which is a divergent function. Outgoing quasi-normal modes are divergent at radial infinity, while ingoing ones tends exponentially to zero as the radius grows. Hence, the purely outgoing condition does not give us a correct boundary condition that could be satisfied at radial infinity. In principle, the purely outgoing quasi-normal mode condition could be imposed at a very distant point, but because of the quick convergence of the ingoing signal, which tends exponentially to zero at radial infinity, every small numerical error in the imposition of this behavior will be amplified as we approach the border of the star, resulting in a mixture of outgoing with ingoing waves. The completely different asymptotic behavior of the outgoing and ingoing quasi-normal modes makes very difficult to obtain quasi-normal modes without any mixture of ingoing waves. So trying to impose this behavior numerically is probably not the best treatment because small numerical deviations far away from the star will translate into big incoming quasi-normal modes contributions at the surface of the star. This is precisely what happens when attempting to calculate strongly damped modes.

We will deal with this problem as we will see below.

III. JUNCTION CONDITIONS

To determine completely the problem, we must study the junction conditions between the interior solution and the exterior solution on the boundary of the star. The junction conditions between two space-times have been considered in classical works by Darmois [49], Lichnerowicz [50], O'Brien and Synge [51], and Israel [52]. Junction conditions for general hypersurfaces have been considered in [53], Symmetry-preserving matchings have been studied in [54], and an analysis of how the induced metric and extrinsic curvature of a hypersurface change, when space-time metric is perturbed to second order and the hypersurface itself is deformed perturbatively to second order, is presented in [55]. Junction conditions for relativistic rotating stars have been considered in [56] and [57]. The junction conditions in surface of energy discontinuity have been considered in [58] to study the influence of phase transition in neutron star quasi-normal modes.

We will impose the usual junction conditions. But, in order to have the possibility to study the influence of small changes in the core-*crust* transition pressure, we will include the more general case in which the star is surrounded by a surface layer of energy density.

We use Darmois conditions, the intrinsic formulation of these junction conditions, which impose certain constrains in the continuity of the fundamental forms of the matching hypersurface S. These conditions are the following: the first fundamental form has to be continuous across S, and the jump in the second fundamental form will be given in terms of the stress-energy tensor of the surface layer [59].

This surface S is defined by the points where the pressure is null, or more generally, constant. As we have seen previously the axial oscillations do not modify the pressure or the density, so the surfaces of constant pressure of the perturbed star are essentially the same as the surfaces of constant pressure of the static star:

$$p = p^{(0)}(r) = const. \tag{16}$$

This condition is equivalent to requiring $r = const. = R$. We calculate a vector normal to these surfaces, n^{μ}, and from it the projector $h_{\mu\nu} = g_{\mu\nu} + n_{\mu}n_{\nu}$ and the projected covariant derivative of the normal vector $\chi_{\mu\nu} = h^{\alpha}_{\mu}h^{\beta}_{\nu}n_{\alpha;\beta}$. Evaluating these tensors at $r = const. = R$, from inside and from outside S, we obtain the first fundamental form and the second fundamental form inside and outside S [59]. We must make a series expansion of these conditions in order to obtain matching relations for each one of the metric functions. We also must expand in spherical harmonics and make a Laplace transformation, in order to obtain the junction of the radial component of the functions.

Let us consider a surface S of constant pressure inside the star, and a surface layer on top of S described by a surface stress-energy tensor of a perfect fluid of the following form:

$$T^{\mu\nu}_{S}(R) = \varepsilon u^{\mu}_{S}(R) u^{\nu}_{S}(R), \tag{17}$$

where, S is defined by the points where $r = const. = R$, ε is the surface energy density of the fluid moving in S, and $u^{\mu}_{S}(R)$ is its velocity. The continuity of the first fundamental form gives us two conditions: the continuity of ν

$$\nu_{int} = \nu_{ext}, \tag{18}$$

and the continuity of perturbation function Z:

$$Z^{lm}_{int} = Z^{lm}_{ext}. \tag{19}$$

The second fundamental form conditions impose a jump in the pressure if $\varepsilon \neq 0$. Let the pressure in the inner part of the surface S, be p_{int}, and in the outer part be p_{ext} with $p_{ext} < p_{int}$.

Making the same steps as with the first fundamental form, we obtain the following conditions for the zero order functions:

$$M_{ext} = M_{int} + 4\pi R^2 \sqrt{1 - \frac{2M_{int}}{R}}\,\varepsilon - 8\pi^2 R^3 \varepsilon^2, \tag{20}$$

$$\frac{M_{ext} + 4\pi R^3 p_{ext}}{R^2\sqrt{1 - \frac{2M_{ext}}{R}}} - \frac{M_{int} + 4\pi R^3 p_{int}}{R^2\sqrt{1 - \frac{2M_{int}}{R}}} = 4\pi\varepsilon. \tag{21}$$

In this work we will consider $p_{ext} = 0$. That is, the surface of star with pressure $p = p_{int}$ is being matched directly to the empty exterior surface of the star, in which case, M_{ext} is just the Schwarzschild mass M. If we choose p_{int} as the core-*crust* transition pressure, this matching condition is equivalent to approximating exterior layers of the star to a surface layer energy density that envelops the core of the star (surface *crust* approximation). The equation (20) can be interpreted as giving the total mass of the star to zero order (M_{ext}), as the addition of three terms, the first one representing the core mass ($M_{int} \equiv 4\pi \int_0^R \rho r^2 dr$), the second one representing the mass of the *crust* and the third one being a negative bounding energy term. The radius of the resulting configuration will be the radius of the core of the star. Equation (21) can be seen as a condition for the determination of the radius of the core of the star when approximating the *crust* of the star to a thin surface energy density.

In the surface *crust* approximation, these relations allow us to use the core-*crust* transition pressure p_{int}, as a new parameter of the resulting configuration.

Up to first order in the perturbative expansion we obtain junction conditions for the axial functions. Essentially we obtain the following condition for the derivative of the Z function:

$$\frac{dZ^{lm}}{dr}|_{ext} = \frac{e^{\lambda_{ext}}}{e^{\lambda_{int}}}\frac{dZ^{lm}}{dr}|_{int} + \left[\frac{e^{\lambda_{ext}}}{e^{\lambda_{int}}} - 1\right]\frac{Z^{lm}}{R}. \tag{22}$$

Together with condition (19) we have enough information to perform correctly the matching of the perturbation.

Let us note that, the usual treatment without surface crust approximation is recovered by making in the previous conditions $p_{int} = p_{ext} = 0$ and $\varepsilon = 0$, in which case the continuity of the metric functions and of their derivatives is obtained. This is what we do in almost all the paper except in the final part of the results section, where the influence of the changes in the core-crust transition pressure is analyzed.

Because the junction conditions for the axial perturbations (19) and (22) are homogeneous in Z, we have a freedom in the global multiplicative factor (the free coefficient from equation (11)). Back to the problem of the determination of the purely outgoing quasi-normal modes, note that now we have sufficient conditions in order to solve the problem: regularity at the origin for the interior perturbation, asymptotic behavior for the exterior one, and matching conditions for both the function and the first derivative of the perturbation.

IV. NUMERICAL METHOD

In this section we will explain the numerical method we use to obtain outgoing quasi-normal modes of realistic stars. We implement this method into different Fortran programs and routines, making use of the Colsys package [60] to solve numerically the differential equations. The advantage of this package is that it allows the utilization of quite flexible multi-boundary conditions, that as we will see in the following sections, are important in our method of quasi-normal mode determination. On the other hand, Colsys allows to construct an adaptative mesh of points depending of the precision we would like to achieve. In this manner, the more precision we need on the perturbation function, the more points Colsys introduces into the mesh. As we will see, the static solution is calculated at the same time as the perturbation, so the static solution functions will be also adapted to the precision we require to the Regge-Wheeler function. Colsys also allows the use of the continuation method: we can use as an initial guess for a new numerical solution another numerical solution which parameters are close enough to the parameters of the new solution.

We will start explaining how the outgoing modes are determined in the exterior region of the metric.

A. Calculation of outgoing quasi-normal modes outside the star

As it has been introduced in previous sections, quasi-normal modes has two main numerical problem. Quasi-normal modes present an oscillating part given by the real part of the eigen-frequency, that remains towards infinity, as can be seen in relation (13). Also, quasi-normal modes diverge towards spatial infinity because of their pure outgoing wave behavior.

In order to deal with these two main issues we will follow [45]-[46], using the phase function together with a rotation of the radial coordinate into the complex plane.

The phase function (logarithmic derivative of the Z function),

$$g = \frac{Z'}{Z}, \tag{23}$$

does not oscillate towards asymptotic infinity. Even more, note that the asymptotic behavior of the phase, considering a general combination of outgoing and ingoing waves is:

$$g \to i\omega \frac{Ae^{i\omega r} - Be^{-i\omega r}}{Ae^{i\omega r} + Be^{-i\omega r}}. \tag{24}$$

When r is real, there are several possibilities. If the mode is purely ingoing, B=0, then $g \to i\omega$. If the mode is purely outgoing, $A = 0$, or if it is a mixture, $A \neq 0$, then $g \to -i\omega$. Although the phase allows us to eliminate the oscillation, we can not distinguish between the mixed incoming and outgoing waves and the purely outgoing ones. The equation for the phase can be written as:

$$\frac{dg}{dr} + g^2 + \tfrac{\omega^2 r^2}{(2-2M)^2} + \tfrac{2M}{r(r-2M)} g - \tfrac{l(l+1)r-6M}{r^4(r-2M)} = 0. \tag{25}$$

As we will see, the phase function has all the information we need to obtain the quasi-normal mode, provided enough junction conditions.

The divergence problem can be avoided by rotating the radial coordinate into the complex plane. This technique of complexification of the integration variable is called Exterior Complex Scaling [61–63]. An analytical extension of the g function, which is a function of r, is made into a g function that is dependent of the generalized complex coordinate. This new function has no physical meaning, but the eigen-values obtained by integrating the equation along the extended radius will remain unaltered.

We parameterize the complex coordinate along a line in the complex plane. We will take a straight line with an angle α with respect the real axis.

$$r = R + ye^{-i\alpha}, \tag{26}$$

with $y \in [0, \infty)$. The g function has the same limits in the case of a purely outgoing or a purely ingoing wave than with the real coordinate. But the mixed waves now depend on the angle of the path of integration α. It can be demonstrated that a mixed ingoing-outgoing wave now presents the following asymptotic behavior for its phase:

$$\omega_{\Re} \sin\alpha + \omega_{\Im} \cos\alpha > 0 \Rightarrow g \to -i\omega, \tag{27}$$

$$\omega_{\Re} \sin\alpha + \omega_{\Im} \cos\alpha < 0 \Rightarrow g \to i\omega. \tag{28}$$

If $\omega_{\Re} \sin\alpha + \omega_{\Im} \cos\alpha = 0$, that is, when $\alpha = -\arctan \frac{\omega_{\Im}}{\omega_{\Re}}$ then the phase become an oscillatory function. This limit line L is parallel to the anti-Stokes line. This path is not useful as our objective is to compactify in order to control completely the boundary conditions. The interesting part of the plane is beyond the line L, because in this region the asymptotic behavior of the purely ingoing waves are exactly the same as the asymptotic behavior of the mixed waves, $g \to i\omega$. In other words, beyond the line L the asymptotic behavior of the outgoing waves $g \to -i\omega$, prohibits any ingoing wave contribution. So now, if we compactify the parameter y by defining $x = \frac{y}{y+1}$, we can impose at infinity ($x = 1$), the boundary condition $g|_{x=1} = -i\omega$. This boundary condition impose to the obtained solution a purely outgoing wave behavior.

In our method, the angle of the integration path is treated as a free parameter of the solution. This angle can be adjusted appropriately to increase precision and integration time, but always remaining in the region where $g \to -i\omega$. Exterior Complex Scaling with variable angle is widely used in other contexts like atomic and molecular physics, where it gives excellent results [64].

The use of the phase and Exterior Complex Scaling with variable angle allows us to compactify, so we can impose the outgoing quasi-normal mode behavior as a boundary condition at infinity without using any cutoff for the radial coordinate.

Note that the equation we must solve now is a first order equation for a complex function. So we have two first order differential equations for two real functions, $g_{\Re}$ and $g_{\Im}$, together with these two boundary conditions: $g_{\Re}|_{x=1} = \omega_{\Im}$ and $g_{\Im}|_{x=1} = -\omega_{\Re}$. So we can obtain a phase function given a pair of values $(\omega_{\Re}, \omega_{\Im})$. We still need the interior part of the quasi-normal mode to determine if this pair of values corresponds to an eigenfrequency or not.

B. Calculation of quasi-normal modes inside a realistic star

Inside the star the Regge-Wheeler equation (8) can be solved without any problem. The perturbation function is oscillating, but the number of oscillations will be finite between $r = 0$ and $r = R$.

To obtain the perturbation function, we need to solve the equations for the zero order functions (4), (5) and (6). To do so, we integrate them with the proper boundary conditions: regularity at the origin and junction conditions (20), (21), using a realistic equation of state.

In order to have the border of the star perfectly under control, we introduce the radius of the star as a function with its own differential equation (constant everywhere inside the star) into the complete system of equations. In principle the interior of the star is a free boundary problem, where the border of the star is obtained where the pressure vanishes. Using the radius as an unknown function allow us to integrate the configuration imposing physical conditions on the boundaries, and obtain the radius as a result in the same manner as one obtains the mass. Colsys is the appropriated way of solving the problem, because Colsys allows to solve differential equations with quite general boundary conditions.

To implement the equation of state we use a piece-wise polytrope approximation, done by Read et al [17]. In this approximation the equation of state is approximated by a polytrope in different density-pressure intervals. For densities below the nuclear density, the SLy equation of state is considered. For higher densities three different regions are used. Then six parameters are needed to model the equation of state: two dividing densities, three adiabatic indices and a value of the pressure at an endpoint of one of the intervals. The piece-wise polytrope approximation is done in [17] for 34 different equations of state, minimizing the error. We have implemented into our routines this approximation for all these equations of state so that once it is selected, the programs read the corresponding 6 parameters and Colsys begins the integration, applying each polytrope to the corresponding density intervals.

As we commented previously, Colsys uses an adaptative mesh of points to generate the solutions, so that if more precision is needed in a certain region of integration, Colsys automatically generates more points there. Because the Regge-Wheeler equation depends on the pressure and mass, this feature is very interesting because allows the Z function to have more points in specially complicated regions where, for example, the pressure drops quickly to zero, increasing the precision in the calculation of the quasi-normal mode. To take advantage of this, we decide to integrate together the zero order and the Regge-Wheeler equation. In this way, we allow Colsys to generate more points in the zero order functions if we require a more precise result in our quasi-normal modes. Colsys allows the use of different tolerances for each function, so different precisions can be achieve in the zero order or in the perturbation functions if necessary.

The Regge-Wheeler equation is a second order equation for a complex function Z. That is, we need to solve two second order equations for two real functions $Z_{\Re}$ and $Z_{\Im}$. We need two boundary conditions for each one of the functions.

We must impose the regularity condition at the origin. Numerically the condition $Z = 0$ is not very constringent, so we choose to redefine the function. Because we are in l=2 modes, we define

$$\hat{Z} = Z/r^3, \tag{29}$$

so that we integrate the equation for $\hat{Z}$. We choose the following two boundary conditions at the origin

$$\hat{Z}' = 0. \tag{30}$$

These conditions impose a regular behavior at the origin. We still need another two conditions. The remaining boundary conditions must guarantee somehow that the matching between the interior and the exterior solutions correspond to an outgoing quasi-normal mode. To determine such solution, we use what we call the *determinant method*.

C. Determination of quasi-normal modes using the Junction Conditions

In order to test if for a certain couple of values $(\omega_{\Re}, \omega_{\Im})$ the obtained solutions are a quasi-normal mode, we must check that the boundary conditions (19) and (22) are satisfied. We use these junction conditions to determine the quasi-normal using the following method:

A general solution to equation (8), once the 2 regularity conditions are imposed, can be obtained by generating to independent solutions and combining them. Note that we still have the free scale factor, so we can obtain the independent solutions by generating two solutions with different internal phases i.e. different $Z_{\Re}/Z_{\Im}$ relation. For example we generate a solution A with $Z^A_{\Re}|_{r=R} = 1$ and $Z^A_{\Im}|_{r=R} = 2$ and another solution B with $Z^B_{\Re}|_{r=R} = 2$ and $Z^B_{\Im}|_{r=R} = 1$. The obtained solutions Z^A and Z^B could be combined to generate any solution $Z = C_A Z^A + C_B Z^B$, where C_A and C_B are two constants.

From the integration of each particular solution we will obtain the value of the derivative at the border of the star, $\frac{dZ^A}{dr}|_{r=R}$ and $\frac{dZ^B}{dr}|_{r=R}$. These values of the Regge-Wheeler function correspond to the interior values of the matching conditions (those obtained in the interior face of the matching surface at $r = R$). Let us rewrite these in the following form, to make it explicit where they are evaluated, if in the outer face of the surface (+) or the inner part (-):

$$Z^A|_{r=R} \equiv Z^A(-), \tag{31}$$

$$\frac{dZ^A}{dr}|_{r=R} \equiv \frac{dZ^A}{dr}(-), \tag{32}$$

and the same for the solution B.

From the boundary condition (19) we know that on the outside face the Regge-Wheeler function must have the same values as the solution on the inside. Outside the star we have calculated the phase, so no value on the surface of the star is imposed to the exterior part of the quasi-normal mode. We use the junction condition (19) to obtain that value. So we have:

$$Z^A(+) = Z^A(-) = 1 + 2i, \tag{33}$$

$$Z^B(+) = Z^B(-) = 2 + i. \tag{34}$$

The values of the derivatives of the Regge-Wheeler functions on the inner face of the surface are obtained numerically from the integration of the Regge-Wheeler equation inside the star: $\frac{dZ^A}{dr}(-)$ and $\frac{dZ^B}{dr}(-)$. But we also need the value of the derivative of the Regge-Wheeler function outside the star. This is easy to obtain from the phase function g outside the star. From the integration of the phase of the Regge-Wheeler function outside the star we have $g|_{x=0} = g(+)$, the phase evaluated on the outer face of the matching surface. By doing the following calculation we obtain the exterior derivative:

$$\frac{dZ^A}{dr}(+) = Z^A(+)g(+), \frac{dZ^B}{dr}(+) = Z^B(+)g(+). \tag{35}$$

This step can be done because we are imposing the continuity of the Regge-Wheeler function for each one of the solutions calculated inside the star, solutions A and B. But this can be perfectly achieved because we still have the freedom in the scale factor for the Regge-Wheeler function outside of the star.

Now that the exterior derivative is calculated, we have all the necessary data to evaluate the junction condition (22) (The necessary values of the zero order functions can be evaluated using the zero order junction conditions). Continuity of particular solutions A and B grants the continuity of the composed solution. The matching (22) must be done on the composed solution. The condition can be written as:

$$\begin{aligned}&\left[C_A \frac{dZ^A}{dr}(+) + C_B \frac{dZ^B}{dr}(+)\right] - \\ &\frac{e^{\lambda(+)}}{e^{\lambda(-)}} \left[C_A \frac{dZ^A}{dr}(-) + C_B \frac{dZ^B}{dr}(-)\right] - \\ &\frac{1}{R}\left[\frac{e^{\lambda(+)}}{e^{\lambda(-)}} - 1\right]\left[C_A Z^A(+) + C_B Z^B(+)\right] = 0.\end{aligned} \tag{36}$$

This condition can be rewritten in matrix form. Note that the Regge-Wheeler function is a complex number. Both the real part and the imaginary part of relation (36) must be null. In other words:

$$M \begin{pmatrix} C_A \\ C_B \end{pmatrix} = 0, \tag{37}$$

with M a matrix which components could be written as:

$$M^i_j = \frac{dZ^i_j}{dr}(+) - \frac{e^{\lambda(+)}}{e^{\lambda(-)}}\frac{dZ^i_j}{dr}(-) - \frac{Z^i_j(-)}{R}\left[\frac{e^{\lambda(+)}}{e^{\lambda(-)}} - 1\right], \tag{38}$$

where $i = \{A, B\}$ and $j = \{\Re, \Im\}$. Because constants C_A and C_B can not be zero at the same time, the quasi-normal mode condition becomes

$$det(M) = 0. \tag{39}$$

The determinant can be calculated numerically from the integrated solutions. For each couple of values $(\omega_\Re, \omega_\Im)$ we can generate interior and exterior solutions, and then calculate the determinant. In principle it will be distinct from zero, but when $\omega_\Re$ and $\omega_\Im$ correspond to a quasi-normal mode eigen-frequency, the determinant will be zero. Because the boundary conditions and junction conditions are only accomplished when we have a outgoing quasi-normal mode, the determinant will be zero if and only if the eigen-value ω corresponds to an outgoing quasi-normal mode.

An important new feature is the use of the continuation method, which allows to use as initial guess solution a previously generated numerical solution. This translates into better convergence times and precision. We start guessing with some values for $\omega_\Re$ and $\omega_\Im$, and then we start moving the parameters, using the numerical solution as an initial guess to generate the next solution with the new parameters. This procedure allows us to sweep the complex plane in reasonable times.

So, in a summary, the method is the following one:

First we select an equation of state from the 34 equations implemented from [17]. Choosing a central pressure, a transition pressure and a value of $\omega_\Re$ and $\omega_\Im$, we integrate the static functions with the appropriate boundary conditions together with the Regge-Wheeler function inside of the star, to which we impose regularity at the origin and two different set of boundary conditions at the border of the star. We obtain two independent solutions for Z. Then we integrate the exterior solution (the phase function) over a rotated spatial coordinate (which is compactified) with an angle beyond the anti-stokes line (this angle can be changed in order to optimize the convergence time and precision of the phase). Imposing the outgoing quasi-normal mode condition, which in this coordinate is well defined, we obtain an outgoing phase function. Now, reading the numerical values from the results, we evaluate the determinant.

We must explore the plane $(\omega_\Re, \omega_\Im)$ looking for null determinants. This process can be automated so that the program looks for minimums of the determinant on the plane. Colsys needs an initial guess solution in order to start the integration algorithm. To generate the first

TABLE I: Frequency and damping time of the trapped modes (t), the spatial modes and the interface modes (i), in central density units, for axial l=2 modes, $2M/R = 0.885$.

$\omega_{\Re}$	$\omega_{\Im}$	$\omega_{\Re}$	$\omega_{\Im}$
(t)0.21386387	$2.4320459 \cdot 10^{-9}$	1.68347876	$6.0243716 \cdot 10^{-2}$
(t)0.29101153	$7.7472523 \cdot 10^{-8}$	1.76704836	$6.1930099 \cdot 10^{-2}$
(t)0.36799864	$1.0725279 \cdot 10^{-6}$	1.85066583	$6.3390024 \cdot 10^{-2}$
(t)0.44463493	$9.5187522 \cdot 10^{-6}$	1.93429817	$6.4699961 \cdot 10^{-2}$
(t)0.52063903	$6.3393194 \cdot 10^{-5}$	2.01793447	$6.5897686 \cdot 10^{-2}$
0.59557900	$3.3806006 \cdot 10^{-4}$	2.10157798	$6.7019361 \cdot 10^{-2}$
0.66896067	$1.4322666 \cdot 10^{-3}$	2.18522398	$6.8080510 \cdot 10^{-2}$
0.74090953	$4.5080077 \cdot 10^{-3}$	2.26888071	$6.9098878 \cdot 10^{-2}$
0.81280272	$1.0135742 \cdot 10^{-2}$	2.35254774	$7.0076042 \cdot 10^{-2}$
0.88590397	$1.7259264 \cdot 10^{-2}$	2.43622599	$7.1018102 \cdot 10^{-2}$
0.96037307	$2.4480195 \cdot 10^{-2}$	(i)1.45115909	$5.4011419 \cdot 10^{-2}$
1.03608110	$3.1027484 \cdot 10^{-2}$	(i)1.73433905	$1.3945066 \cdot 10^{-2}$
1.11308152	$3.6685221 \cdot 10^{-2}$	(i)2.01106806	$2.2902687 \cdot 10^{-2}$
1.19147020	$4.1559313 \cdot 10^{-2}$	(i)2.29393679	$3.1975625 \cdot 10^{-2}$
1.27122330	$4.5838031 \cdot 10^{-2}$	(i)2.57982976	$4.1067802 \cdot 10^{-2}$
1.35219268	$4.9636532 \cdot 10^{-2}$	(i)2.86633683	$5.0155809 \cdot 10^{-2}$
1.43415622	$5.2976144 \cdot 10^{-2}$	(i)3.15274466	$5.9234204 \cdot 10^{-2}$
1.51685560	$5.5841641 \cdot 10^{-2}$	(i)3.43712011	$6.8307813 \cdot 10^{-2}$
1.60003382	$5.8244121 \cdot 10^{-2}$		

solution, we use simple polynomial functions. But once one numerical solution for a particular equation of state is known, Colsys allows the use of these solutions as the initial guess. So once a solution is obtained, another solution can be generated by small modifications of the parameters of the previous solution. The smaller the change in the parameters, the faster the convergence of the programs. The interesting region of the plane $(\omega_{\Re}, \omega_{\Im})$ can be explored by this procedure, looking for null determinants, in a reasonable amount of time.

We have made several tests on our method using simpler equations of state. We successfully reproduce data from previous works. For example in table I we show our results for a star of constant density and $2M/R = 0.885$, in perfect agreement with [46].

In Figures 1 and 2 we show an example of calculated perturbation functions. These functions correspond to a star of $1.4M_{\odot}$, with the high density Sly equation of state. The quasi-normal mode is the first axial mode w_I with frequency $\nu = 8.034kHz$ and damping time $\tau = 29.31\mu s$. In Figure 1 we plot the real and imaginary parts of the two interior solutions for Z vs r. In Figure 2 we plot the real and imaginary parts of the calculated phase function outside the star versus the compactified rotated coordinate x.

In the next sections we will show the results obtained for realistic equations of state.

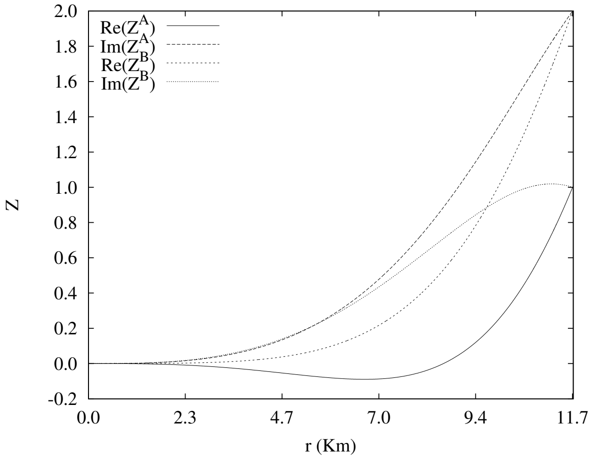

FIG. 1: Example of Regge-Wheeler function inside the star.

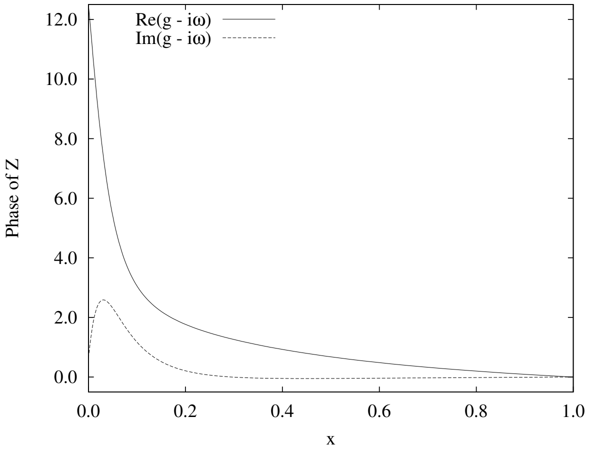

FIG. 2: Example of phase function g outside the star.

V. RESULTS

In this section we present our results for the axial quasi-normal modes of neutron stars with realistic equations of state. From the equations of state implemented using [17], we focus the study on the following four equations of state: the high density SLy [65], a equation of state for plain nuclear matter; ALF4, a hybrid equation of state with mixture of nuclear matter and color-flavor locked quark matter [66]; and two equations of state for mixed nuclear and hyperon matter, GNH3 [67] and BGN1H1 [68]. In Figure 3 we show the different equations of state in the high density region. For lower densities the equation of state used is the Sly [17]. In Figure 4 we show the mass radius relation for these equations of state. For the study of the quasi-normal modes we have considered only stable configurations below the maximum mass of each equation of state. The introduction of a hyperon core changes the mass radius relation and we will see that this also has an imprint on the quasi-normal mode spectrum of these configurations.

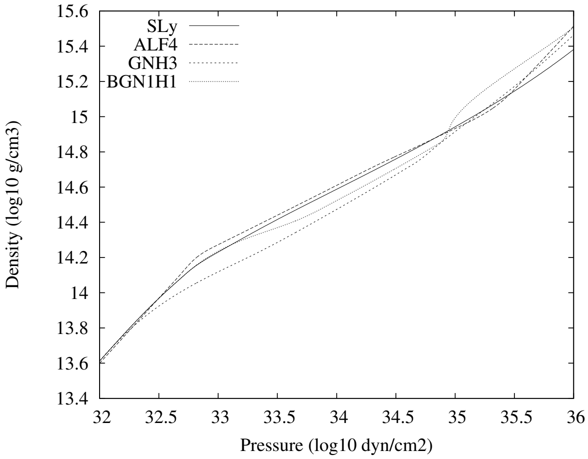

FIG. 3: Density versus pressure in logarithmic scale for the four equations of state considered, in the high density region.

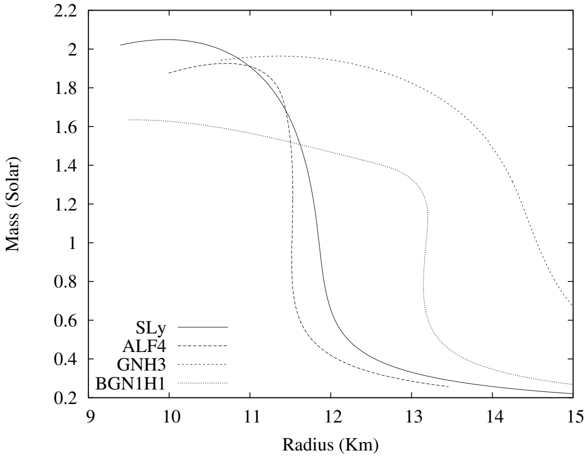

FIG. 4: Mass vs radius relation for the four equations of state considered.

We start studying the first w modes, in order to examine the imprint of each equation of state in the quasinormal modes.

In Figure 5 we plot the frequency of the fundamental wI mode as a function of the compactness of the star, M/R, for the different equations of state. We plot from compactness 0.1 up to the maximum mass configuration, so we consider only stable stars. We observe that for the wI modes the presence of hyperon condensates has a clear impact on the frequencies of the fundamental w-modes, while there is no significant difference between pure nuclear matter and mixed quark-nuclear states. Note how the hyperon core is changing the frequency relation for high compactness configurations, increasing with M/R above a given compactness. In Figure 6 we make a similar plot for the damping time of these configurations.

In order to use future observations of gravitational waves to estimate the mass and the radius of the neutron star, as well as to discriminate between different families of equations of state, we obtain empirical relations between the frequency and damping time of quasi-normal modes and the compactness of the star, following [4],[69], [70] and [20]. In Figure 7 we present the frequency of the fundamental mode scaled to the radius of each configuration. It is interesting to note that even with this scaling, the softer equations of state that include hyperon matter, and in particular, the BGN1H1 equation of state, present a quite different behavior than SLy and ALF4 equations of state.

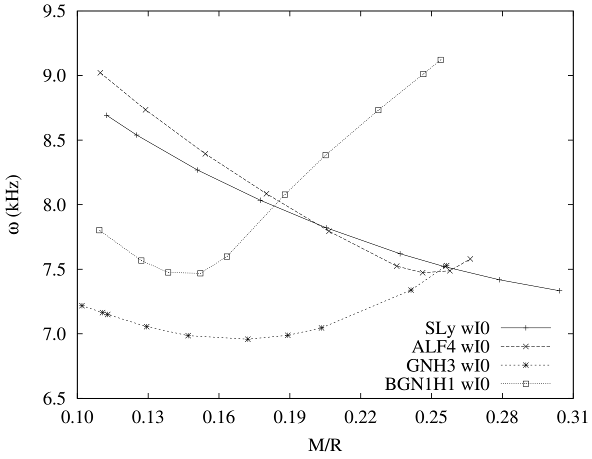

FIG. 5: Frequency of the fundamental wI mode vs M/R.

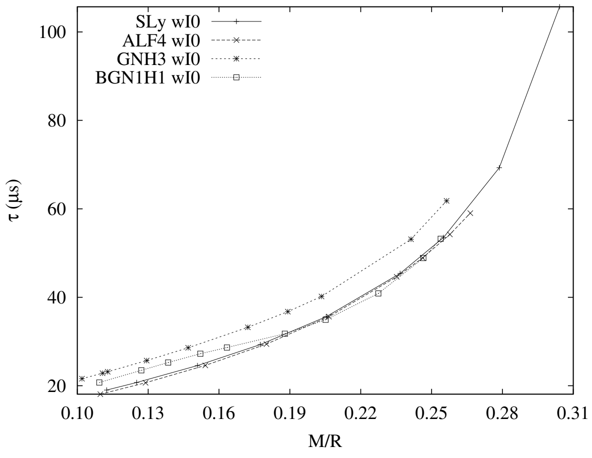

FIG. 6: Damping time of the fundamental wI mode vs M/R.

A linear fit can be made to these last two equations of state. We fit to

$$\omega(Khz) = \frac{1}{R(Km)}\left(A\frac{M}{R}+B\right). \tag{40}$$

TABLE II: Fitting for the wI0 modes. Parameters A and B correspond to the linear empirical relation for the frequency (40). Parameters a,b and c correspond to the quadratic empirical relation for the damping time (41).

wI0 modes	SLy	ALF4	GNH3	BGN1H1
A	-148.7 ± 4.5	-141.4 ± 1.2	-122.1 ± 1.4	-
B	119.8 ± 1.0	118.40 ± 0.25	116.67 ± 0.25	-
χ^2	0.760	0.039	0.057	-
a	-1221 ± 22	-1158 ± 26	-1444 ± 23	-1690 ± 49
b	365.1 ± 9.3	345.3 ± 9.8	425.4 ± 8.3	506 ± 18
c	21.63 ± 0.89	23.06 ± 0.88	17.87 ± 0.68	11.2 ± 1.6
χ^2	0.050	0.028	0.027	0.084

TABLE III: Fitting for the wI1 modes. Parameters A and B correspond to the linear empirical relation for the frequency (40). Parameters a,b and c correspond to the quadratic empirical relation for the damping time (41).

wI1 modes	SLy	ALF4	GNH3	BGN1H1
A	-689.5 ± 5.2	-688.8 ± 6.8	-736.5 ± 6.8	-779.4 ± 6.8
B	312.5 ± 1.1	313.5 ± 1.4	317.2 ± 1.4	323.3 ± 1.4
χ^2	0.997	1.236	0.372	1.986
a	-1843 ± 55	-1857 ± 110	-2062 ± 25	-1771 ± 123
b	650 ± 23	654 ± 42	690.9 ± 8.9	582 ± 45
c	14.3 ± 2.2	14.2 ± 3.8	13.10 ± 0.73	21.1 ± 3.9
χ^2	0.311	0.510	0.0252	0.393

In Table II we present the fitting parameters A,B for each one of the equations of state studied. For the Sly and for the ALF4 equations very similar results are obtained. The empirical parameters for SLy and ALF4 are compatible with the empirical relation obtained by Benhar et al [70] for six equations of state.

For the GNH3 equation of state we still obtain a linear relation, but with different parameters as can be seen in Table II. The introduction of hyperon matter is affecting the empirical relation.

For the BGN1H1 equation of state the relation of the scaled mass with the compactness is not even linear, as can be seen in Figure 7. Our results show that the introduction of hyperon matter changes the dependence of the frequency with the compactness. For compactness bigger than 0.18, the difference between the equations of state with and without hyperon matter is quite important. This feature could be used applying the technique from [69] to test the presence of hyperon matter inside neutron stars. Indications in this direction have been obtained in a recent work ([24]). Chatterjee and Bandyopadhyay have studied the wI0 mode for other equations of state involving hyperons as well as Bose-Einstein condensates of antikaons obtaining that exotic matter can be distinguish from nucleons only matter.

In Figure 8 we present the damping time of the fundamental mode scaled to the mass of each configuration. In this case, the results can be fitted to a empirical quadratic relation on M/R, as follows:

$$\frac{1}{\tau(\mu s)} = \frac{1}{M(M_\odot)}\left[a\left(\frac{M}{R}\right)^2 + b\frac{M}{R} + c\right]. \qquad (41)$$

In Table II we present the fitting parameters a,b and c. Note that for SLy and ALF4 the fits are quite similar, and in accordance with the results obtained in ([70]). For GNH3 and BGN1H1 equations of state, although the result are well fitted to a quadratic relation, the coefficients are very different from those obtained for Sly and ALF4 equations of state. As occurred with the frequency, this feature could be used to test the presence of hyperon matter in the equation of state.

Considering the results obtained for the fundamental modes of Sly and ALF4 equations of state, it is not possible to distinguish between mixed quark-nuclear matter composition and pure nuclear matter composition.

We have developed a similar study with the first excited wI-mode. In Figures 9 and 10 we plot the scaled frequency and damping time for these modes. The same empirical relations (40, 41), with different parameters can be found. In Table III we present the corresponding empirical parameters.

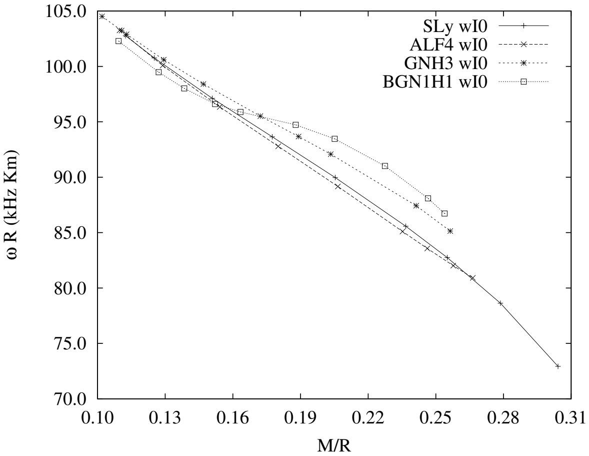

FIG. 7: Scaled frequency of the fundamental wI mode vs M/R.

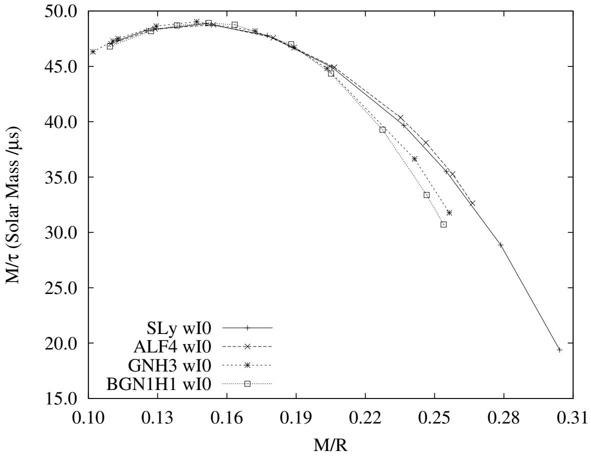

FIG. 8: Scaled damping time of the fundamental wI mode vs M/R.

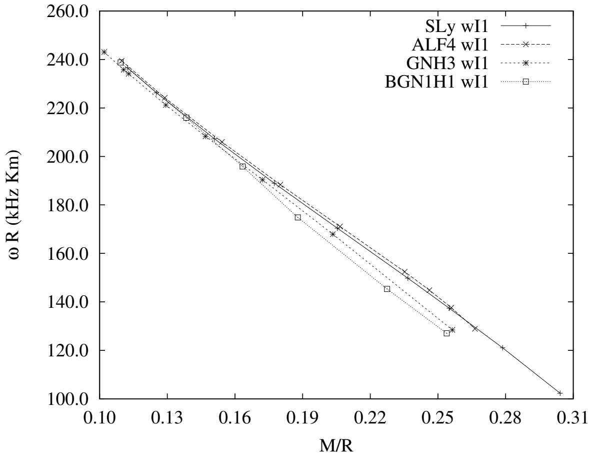

FIG. 9: Scaled frequency of the first excited wI mode vs M/R.

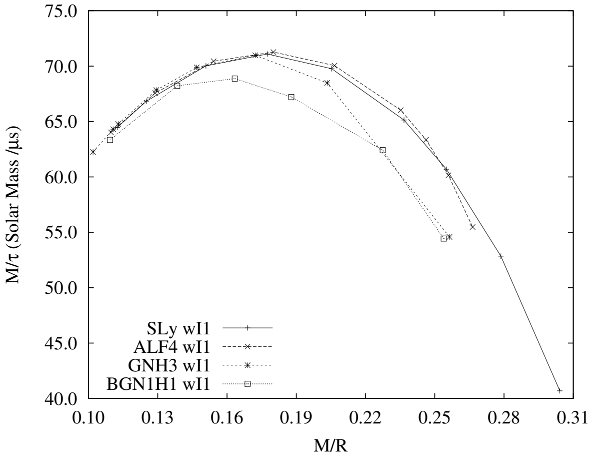

FIG. 10: Scaled damping time of the first excited wI mode vs M/R.

Concerning the frequency of the wI1 modes, although the linear relation for the scaled frequency is well satisfied for all the equations of state, the slope is slightly steeper for the GNH3 and BGN1H1.

Concerning the damping time of the wI1 modes, the situation is quite similar to the frequency. The quadratic relation is very well satisfied, but note that the parameters of the quadratic relation are very sensitive to the presence of hyperon matter.

In Figure 11 we plot the frequency of the fundamental wII mode scaled with the mass versus the metric function $e^{2\lambda}$. It can be seen that for all the equations of state studied, there is a minimal compactness, below which the wII mode do not exist. The scaled frequency is quite linear with $e^{2\lambda}$ nearby this minimal compactness. Our numerical scheme allows us to obtain explicitly these limit configuration with vanishing real part of the mode with a precision of the order of 10^{-5}. For the SLy and ALF4 equations of state, the limit configuration has compactness $M/R = 0.1063$. For the GNH3 equation of state the limit configuration has compactness $M/R = 0.1051$, and for the BGN1H1, $M/R = 0.1061$. Note that these configurations for which the fundamental wII vanishes has a compactness quite independent of the equation of state. These configurations were conjectured by Wen et al in [25]. Although in this work they were not able to obtain explicity the limit configuration, so the compactness of the limit configuration were obtained by extrapolation. Our results are in agreement with their extrapolation.

In Figure 12 we show the damping time of the wII mode scaled with the mass. Although for low compactness the damping time is quite independent of the equation of state and linear in M/R, for compactness above 0.18 it is very sensitive to the presence of hyperon matter, changing completely the linear behavior. The damping time does not vanish in the limit compactness as the frequency does. By the contrary it tends to a limit τ dependent of the equation of state.

We would like to remark the similitude between the

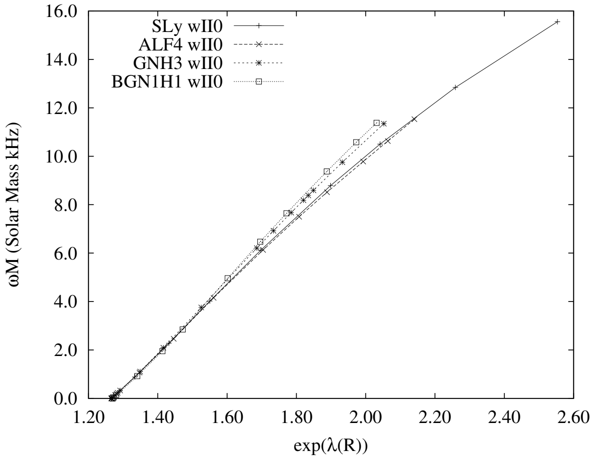

FIG. 11: Scaled frequency of the fundamental wII mode vs $e^{\lambda(R)}$.

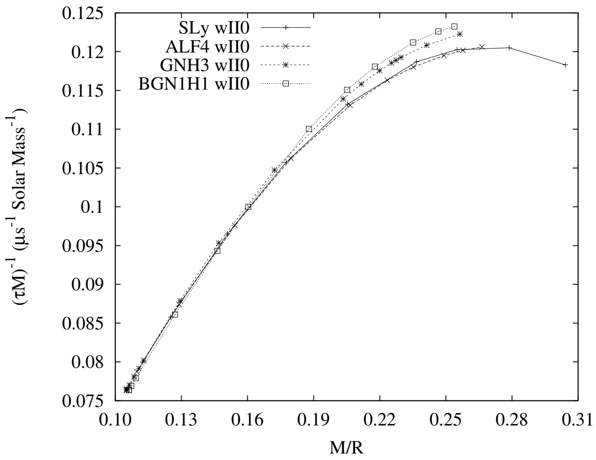

FIG. 12: Damping time of the fundamental wII mode vs M/R.

SLy and ALF4 frequencies and damping times for every neutron star mass. Their first w-modes are practically indistinguishable. In fact, it has been shown that for realistic equations of state like the ALF4, for mixed nuclear and quark matter, the mass-radius relation of the stars is quite similar to the mass-radius relation of stars composed of pure nuclear matter [66]. This makes impossible to decide if a star presents quark matter in their interior by measuring the mass and the radius. Our results show that neither the observation of the frequencies or damping times of the axial w-mode spectrum of neutron stars could allow us to decide if the equation of state presents mixed nuclear-quark matter states. On the contrary, the determination of the frequencies could tell us if there are hyperon condensates inside the star.

Let us present an empirical relation between the real part and the imaginary part of the modes, that seems to be independent of the equation of the state. As far as we know this has not been obtained before. In Figure 13 we plot, for multiple configurations and all the equations of state studied, the real part versus the imaginary part of the quasi-normal mode. The modes are in units of the central pressure. So to obtain the modes with correct units one have to use the following formulas:

$$\omega(Khz) = \sqrt{p_c(cm^{-2})}\frac{c}{1000}\frac{1}{2\pi}\omega_{Re},$$
$$\tau(\mu s) = (\sqrt{p_c(cm^{-2})}\frac{c}{10^6}\omega_{Im})^{-1}, \qquad (42)$$

where c is the speed of light in cm/s. It is interesting to note the following universal relations:

For the fundamental wI modes, our results of the imaginary part versus the real part can be fitted to a quadratic relation as follows:

$$\omega_{Im} = (-1.98 \pm 0.22) + (0.497 \pm 0.030)\omega_{Re} + (0.0193 \pm 0.0008)\omega_{Re}^2, \qquad (43)$$

with $\chi^2 = 0.0624$.

For the first excited wI mode, we obtain the following fit:

$$\omega_{Im} = (-1.33 \pm 0.22) + (0.495 \pm 0.014)\omega_{Re} + (0.00153 \pm 0.00018)\omega_{Re}^2, \qquad (44)$$

with $\chi^2 = 0.118773$. It is almost linear with the real part.

For the fundamental wII mode, the real part is quadratic with the imaginary part. We obtain the following fit:

$$\omega_{Re} = (4.23 \pm 0.27) + (0.170 \pm 0.024)\omega_{Im} + (-0.00524 \pm 0.00041)\omega_{Im}^2, \qquad (45)$$

with $\chi^2 = 0.188$. These relations allows to obtain the ω_{Im} if ω_{Re} is known, recalling relations of this type in other context (Kramers-Kroning relations). From a practical point of view this relation can be used to simplify the numerical calculations to obtain quasi-normal modes for any equation of state, reducing, in our method, the time necessary to find the zeros of the determinant.

We would like to point out that these empirical relations can be used to estimate the central pressure of the neutron star. For instance, if the frequency and the damping time of the fundamental mode of a neutron star are detected, using (42) and (43) we are able to obtain a value for the central pressure p_c. Actually, given the precision of the fit, we can only obtain the order of the magnitude of the central pressure valid for any equation of state. If the mass and the radius of the neutron star have been measured with another method, combining these data with the central pressure, we could test the validity of a particular equation of state, using the mass versus radius relation for it. In Figure 14 we show the axial quasi-normal mode spectrum up to the fifth excited mode of neutron stars with $M = 1.4M_\odot$ for the four equations of state. For stars of this mass the spectrum for SLy and ALF4 almost coincide. Hence,

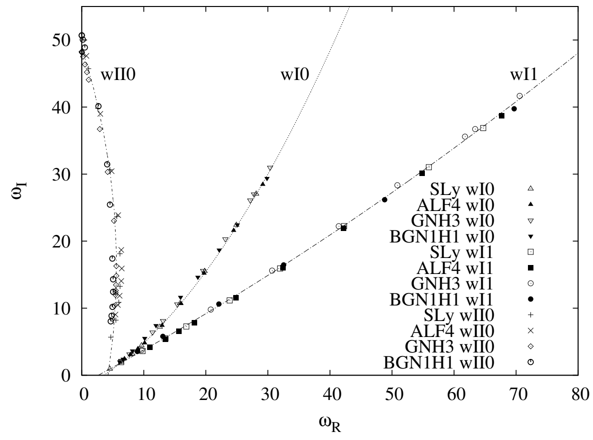

FIG. 13: All w-modes in units of the central pressure for the different equations of state and different central pressures.

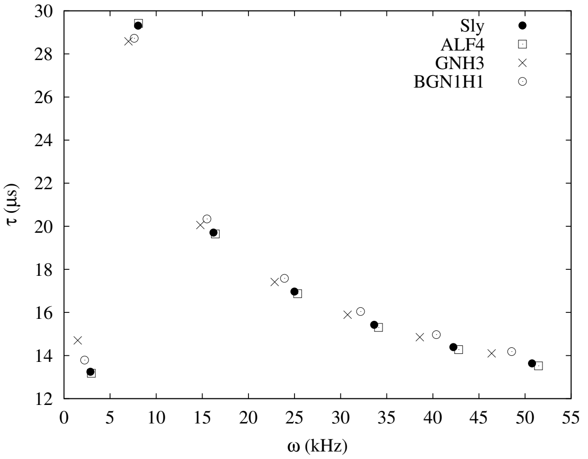

FIG. 14: Axial w-mode spectrum for stars of $1.4M_{\odot}$.

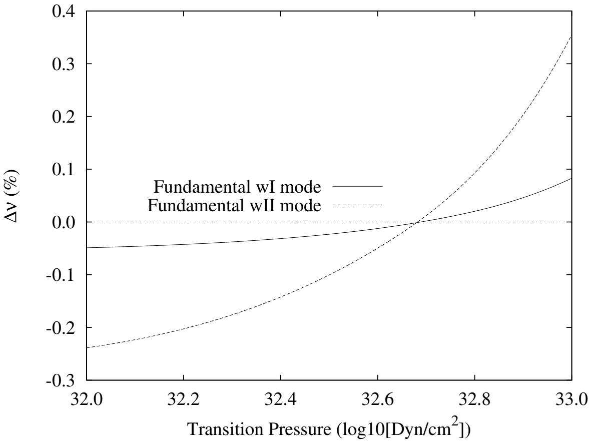

FIG. 15: Variation of the frequency vs the transition pressure.

these equations of state cannot be distinguished up to the fifth mode. The spectrum for equations of state including hyperon matter is slightly different. When the order of the mode increases, the frequency and the damping time of the modes allow to distinguish between neutron stars with and without hyperon matter. So an study of different modes could be used to determine which particle species are populating the inner layers of the star. Finally, we study the effect of core-*crust* transition pressure variations in the quasi-normal mode spectrum using our model of crust as a surface energy density enveloping the core. We will consider the SLy equation of state, for which the core-*crust* transition is found at density $1.29 \cdot 10^{14} g/cm^3$. We construct a star of $1.4M_{\odot}$ with and without a surface energy density enveloping the core of the star at this core-*crust* transition region. We can compare the difference in the fundamental w modes between our approximation of *crust* as a thin shell enveloping the core, and the standard calculation. The result is the following: for the fundamental wI mode, the change in the frequency is 0.07% and the variation in the damping time is -0.02%. For the fundamental wII mode, the changes are bigger. For the frequency 0.3% and for the damping time -0.07%. This indicate that this approximation makes small changes in the w quasi-normal spectrum.

In Figures 15 and 16 we present the influence of core-*crust* transition pressure variation in the fundamental w-modes. We consider an initial neutron star with $1.4M_{\odot}$ and surface energy density at the core-*crust* transition point: $4.8 \cdot 10^{32} dyn/cm^2$. Fixing the central pressure, we variate the core-*crust* transition pressure between $10^{32} dyn/cm^2$ and $10^{33} dyn/cm^2$, and compare with the modes for the initial configuration. In Figure 15 we plot the relative variation in the frequency. It can be seen that the impact of transition pressure variations on the frequency is small, between -0.05% and 0.08% for the fundamental wI mode, and between -0.24% and 0.35% for the fundamental wII mode. In Figure 16 we plot the relative variation in the damping time with a similar result. Transition pressure variations has a small impact on the damping time, between 0.02% and -0.035% for the fundamental wI mode, and between 0.06% and -0.1% for the fundamental wII mode.

VI. SUMMARY

In this paper we have studied the axial w quasi-normal modes for several equations of state. In particular, we consider the influence of the presence of hyperons in the core of the neutron star. We have obtained that, in principle, for enough compact stars we can distinguish between stars with hyperons and stars without hyperons in their core.

In order to do that we have developed a new algorithm, and a new numerical code to calculate w-axial quasi-normal modes for neutron stars with realistic equations of state.

In the exterior of the star we use the phase of the

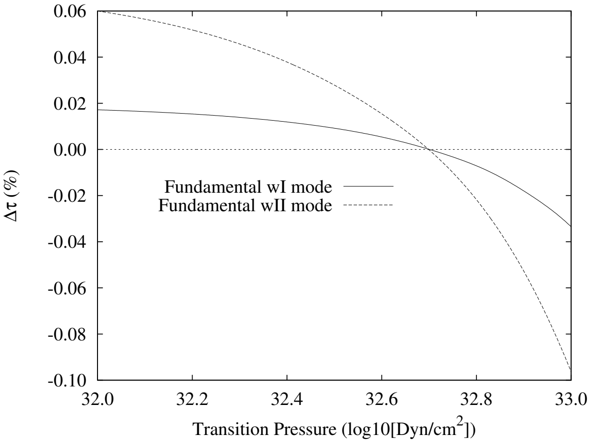

FIG. 16: Variation of the damping time vs the transition pressure.

Regge-Wheeler function, which is not an oscillatory function as the Regge-Wheeler function. In order to generate properly outgoing quasi-normal waves, removing the divergence towards infinity, we have used Exterior Complex Scaling, allowing us to impose constringent enough conditions at infinity by the compactification of the exterior region. This treatment allows us to grant that the exterior solution corresponds to an outgoing wave, without any possibility of incoming wave contamination. What is new in this part of the algorithm is that we allow for a variable angle in the complex scaling, which makes it possible to obtain new modes and better precision than in previous works.

In the interior of the star we obtain the general solution of the Regge-Wheeler equation, as a linear combination of two numerically generated independent solutions for neutron star with realistic equations of state and regularity conditions in the center of the star. Then the interior and the exterior solution have to be matched adequately in the border of the star. Only for some values of the frequency ω and damping time τ it is possible to satisfy these multi-boundary conditions: conditions in the center of the star, in the border of the star and at the spatial infinity. Our algorithm reduces the search for these values of ω and τ to the search of the zeros of the determinant of a matrix evaluated in the border of the star.

A complete study of the junction conditions in a surface of constant pressure (also including the case $p = 0$, the border of the star) has been done using intrinsic Darmois formulation. We include the general case with a surface layer in the boundary that can be used to study situations with a rapid variation in the density (for instance, in the crust-core transition region).

It is interesting to note some technical points of the algorithm: we have used Colsys, a collocation package, to integrate the differential equations given its ability to treat multi-boundary conditions and it has great flexibility available to impose the precision on the different functions. We integrate the background (zero-order) and the perturbation (first-order) at the same time to obtain the precision in the zero order needed to calculate the perturbation with the precision required. Usually for high excited modes the Regge-Wheeler function presents an important number of oscillations inside the star. More precision on the static functions (zero order) is needed, but as the functions are all resolved at once, the programs just adapt the mesh until the convergence criteria is achieved. In order to be able to integrate the zero order and the perturbation at the same time, we have added a trivial equation for the border of the star R. Also, it is interesting to note, that the continuation method is used to generate families of solutions varying slowly a given parameter, and that a large region of the complex plane of ω has been explored looking for zeros of the determinant condition.

One expects that the spectrum of quasi-normal modes has to depend on the equation of the state of the neutron star. Hence, the observation of the spectrum of quasi-normal modes will impose constrains on the equation of the state (EOS). To do that, in an effective manner, it is interesting to have a parameterization of the EOS in terms of a small number of parameters. In this work we have used a piece-wise polytropic approximation by Jocelyn et al. [17], which fits, with a very good precision, a large family of EOS.

To study the influence of the presence of hyperons in the core of the neutron star we concentrate our study in four EOS: SLy (nuclear matter), ALF4 (mixed nuclear and quark matter), GNH3 and BGN1H1 (with hyperon condensates).

We have obtained phenomenological relation for the frequency and damping time with M/R for wI and wII modes indicating that we can not differentiate the results for SLy(nuclear matter) and ALF4 (mixed nuclear and quark matter). But the presence of hyperons in GNH3 and BGN1H1 EOS influence enough the spectrum to make possible to distinguish the spectrum of a star with hyperons and a star without hyperons if the compactness is large enough.

Other interesting result is that we have obtained a new phenomenological relation between the real part and the imaginary part of the frequency of the w quasi-normal modes valid for the four EOS. This relation allows to obtain an estimation of the central pressure of the star independent of the EOS, if the frequency and the damping time of the w fundamental mode of a neutron star is detected.

Also, the precision of our algorithm allows us to construct explicitly the universal low compactness limiting configuration around $M/R = 0.106$ for which the fundamental wII mode vanishes. The existence of this configuration had been conjectured by [25].

Finally, we have studied the influence of changes in the core-*crust* transition pressure obtaining that the influence is very small. The relative changes in the frequency for a variation of the core-*crust* transition from $10^{32} dyn/cm^2$ to $10^{33} dyn/cm^2$ are between 0.02% and −0.035% for the fundamental wI mode, and between 0.06% and −0.1% for the fundamental wII mode. In the damping time the relative changes are between 0.02% and −0.035% for the fundamental wI mode, and between 0.06% and −0.1% for the fundamental wII mode.

Acknowledgments

We thank Prof. Kostas D. Kokkotas for very helpful discussions concerning quasi-normal modes of neutron stars. J.L.B wants to thank also his kind hospitality. Also, we are very grateful to Prof. Gabriel A. Galindo for his help concerning the Exterior Complex Scaling method. This work was supported by the Spanish Ministerio de Ciencia e Innovacion, research project FIS2011-28013. J.L.B was supported by the Spanish Universidad Complutense de Madrid.

---

[1] M. Pitkin, S. Reid, S. Rowan, and J. Hough, Living Reviews in Relativity **14** (2011).
[2] B. Sathyaprakash and B. F. Schutz, Living Reviews in Relativity **12** (2009).
[3] N. Andersson, V. Ferrari, D. Jones, K. Kokkotas, B. Krishnan, J. Read, L. Rezzolla, and B. Zink, General Relativity and Gravitation **43**, 409 (2011).
[4] N. Andersson and K. D. Kokkotas, Physical Review Letters **77**, 4134 (1996).
[5] M. Shibata, K. Taniguchi, and K. b. o. Uryū, Phys. Rev. D **71**, 084021 (2005).
[6] M. Shibata and K. Uryū, Progress of Theoretical Physics **107**, 265 (2002).
[7] R. Oechslin, H.-T. Janka, and A. Marek, A&A **467**, 395 (2007).
[8] T. Hinderer, B. D. Lackey, R. N. Lang, and J. S. Read, Phys. Rev. D **81**, 123016 (2010).
[9] J. S. Read, C. Markakis, M. Shibata, K. b. o. Uryū, J. D. E. Creighton, and J. L. Friedman, Phys. Rev. D **79**, 124033 (2009).
[10] J. Abadie, B. P. Abbott, R. Abbott, R. Adhikari, P. Ajith, B. Allen, G. Allen, E. Amador Ceron, R. S. Amin, S. B. Anderson, et al. (The LIGO Scientific Collaboration), Phys. Rev. D **83**, 042001 (2011).
[11] K. D. Kokkotas and B. Schmidt, Living Reviews in Relativity **2** (1999).
[12] H.-P. Nollert, Classical and Quantum Gravity **16**, R159 (1999).
[13] L. Rezzolla, Black Holes and Relativistic Stars p. 47 (2003).
[14] A. Haensel, P. Potekhin and D. Yakovlev, *Neutron stars: Equation of state and structure*, Astrophysics and space science library (Springer, 2007).
[15] N. Glendenning, *Compact stars: nuclear physics, particle physics, and general relativity*, Astronomy and astrophysics library (Springer, 2000).
[16] H. Heiselberg and M. Hjorth-Jensen, Physics Reports **328**, 237 (2000).
[17] J. S. Read, B. D. Lackey, B. J. Owen, and J. L. Friedman, Phys. Rev. D **79**, 124032 (2009).
[18] L. Lindblom, Phys. Rev. D **82**, 103011 (2010).
[19] O. Benhar, E. Berti, and V. Ferrari, Monthly Notices of the Royal Astronomical Society **310**, 9 (1999).
[20] K. D. Kokkotas, T. A. Apostolatos, and N. Andersson, Monthly Notices of the Royal Astronomical Society **320**, 307 (2001).
[21] O. Benhar, V. Ferrari, and L. Gualtieri, Physical Review D **70**, 124015 (2004).
[22] O. Benhar, Mod.Phys.Lett. **A20**, 2335 (2005).
[23] V. Ferrari and L. Gualtieri, Gen.Rel.Grav. **40**, 945 (2008).
[24] D. Chatterjee and D. Bandyopadhyay, Phys.Rev. **D80**, 023011 (2009).
[25] D.-H. Wen, B.-A. Li, and P. G. Krastev, Phys.Rev. **C80**, 025801 (2009).
[26] T. Regge and J. A. Wheeler, Physical Review **108**, 1063 (1957).
[27] F. J. Zerilli, Phys. Rev. Lett. **24**, 737 (1970).
[28] K. Thorne and A. Campolattaro, Astrophys. J. **149**, 591 (1967).
[29] R. Price and K. Thorne, Astrophys. J. **155**, 163 (1969).
[30] K. Thorne, Astrophys. J. **158**, 1 (1969).
[31] K. Thorne, Astrophys. J. **158**, 997 (1969).
[32] A. Campolattaro and K. Thorne, Astrophys. J. **159**, 847 (1970).
[33] L. Lindblom and S. Detweiler, Astrophys. J. Supplement Series **53**, 73 (1983).
[34] S. Detweiler and L. Lindblom, Astrophys. J. **292**, 12 (1985).
[35] S. Chandrasekhar and V. Ferrari, Proceedings of the Royal Society of London. Series A: Mathematical and Physical Sciences **432**, 247 (1991).
[36] S. Chandrasekhar, V. Ferrari, and R. Winston, Proceedings of the Royal Society of London. Series A: Mathematical and Physical Sciences **434**, 635 (1991).
[37] S. Chandrasekhar and V. Ferrari, Proceedings of the Royal Society of London. Series A: Mathematical and Physical Sciences **434**, 449 (1991).
[38] Y. Kojima, Phys. Rev. D **46**, 4289 (1992).
[39] Y. Kojima, N. Andersson, and K. D. Kokkotas (1995).
[40] K. D. Kokkotas, Monthly Notices of the Royal Astronomical Society **268**, 1015 (1994).
[41] K. D. Kokkotas and B. F. Schutz, Monthly Notices of the Royal Astronomical Society **255**, 119 (1992).
[42] N. Andersson, K. D. Kokkotas, and B. F. Schutz, Monthly Notices of the Royal Astronomical Society **274**, 9 (1995).
[43] S. Chandrasekhar and S. Detweiler, Proceedings of the Royal Society of London. A. Mathematical and Physical Sciences **344**, 441 (1975).

[44] N. Andersson, Y. Kojima, and K. D. Kokkotas, Astrophysical Journal **462**, 855 (1996).

[45] N. Andersson, Proceedings of the Royal Society of London. Series A: Mathematical and Physical Sciences **439**, 47 (1992).

[46] L. Samuelsson, N. Andersson, and A. Maniopoulou, Classical and Quantum Gravity **24**, 4147 (2007).

[47] E. W. Leaver, Proceedings of the Royal Society of London. Series A: Mathematical and Physical Sciences **402**, 285 (1985).

[48] M. Leins, H. P. Nollert, and M. H. Soffel, Phys. Rev. D **48**, 3467 (1993).

[49] G. Darmois, Mémorial des Sciences Mathématiques (Paris:Gauthier-Villars) **25** (1927).

[50] A. Lichnerowicz, *Théories Relativistes de la Gravitation et de l'Electromagnétism* (Maison, Paris, 1955).

[51] S. O'Brien and J. Syngr, Comm. Dublin Inst. Adv. Stud. Ser. A **9**, 1 (1952).

[52] W. Israel, Nuovo Cimento B **B44**, 1 (1966).

[53] M. Mars and J. M. Senovilla, Class.Quant.Grav. **10**, 1865 (1993).

[54] R. Vera, Class.Quant.Grav. **19**, 5249 (2002).

[55] M. Mars, Class.Quant.Grav. **22**, 3325 (2005).

[56] L. M. González-Romero, Phys. Rev. D **67**, 064011 (2003).

[57] M. A. H. MacCallum, M. Mars, and R. Vera, Phys. Rev. D **75**, 024017 (2007).

[58] H. Sotani, K. Tominaga, and K.-i. Maeda, Phys. Rev. D **65**, 024010 (2001).

[59] C. Misner, K. Thorne, and J. Wheeler, *Gravitation*, Physics Series (W. H. Freeman, 1973).

[60] U. Ascher, J. Christiansen, and R. D. Russell, Mathematics of Computation **33**, pp. 659 (1979).

[61] J. Aguilar and J. Combes, Commun. Math. Phys. **22**, 269 (1971).

[62] E. Balslev and J. Combes, Commun. Math. Phys. **22**, 280 (1971).

[63] B. Simon, Commun. Math. Phys. **27**, 1 (1972).

[64] G. Alvarez, R. Damburg, and H. Silverstone, Phys. Rev. A **44**, 3060 (1991).

[65] F. Douchin and P. Haensel, A&A **380**, 151 (2001).

[66] M. Alford, M. Braby, M. Paris, and S. Reddy, Astrophys. J. **629**, 969 (2005).

[67] N. Glendenning, Astrophys. J. **293**, 470 (1985).

[68] S. Balberg and A. Gal, Nuclear Physics A **625**, 435 (1997).

[69] N. Andersson and K. D. Kokkotas, Monthly Notices of the Royal Astronomical Society **299**, 1059 (1998).

[70] O. Benhar, E. Berti, and V. Ferrari, Monthly Notices of the Royal Astronomical Society **310**, 797 (1999).